ORIGINAL PAPER-PRODUCTION ENGINEERING

Quantitative evaluation of water-alternative-natural gas flooding in enhancing oil recovery of fractured tight cores by NMR

Baishuo Liu[1,2] · Chuanjin Yao[1,2] · Yaqian Liu[1,2] · Jia Zhao[1,2] · Zhengdong Lei[3] · Yiran Zhou[1,2] · Yuyuan Song[1,2] · Lei Li[1,2]

Abstract

As the associated gas of tight reservoirs, natural gas is abundant and noncorrosive, which is more suitable for the development of tight oil reservoirs in China. However, the mechanism of gas injection development is unclear, and the gas channeling is serious in tight reservoirs after fracturing. The water-alternating-gas (WAG) flooding is an effective means to delay gas channeling and improve oil recovery. Therefore, it is significant to clarify the mechanism of preventing gas channeling and recovering oil by water-alternation-natural gas (WANG) flooding. The WANG flooding experiments with different water–gas slugs were conducted in non-fracture and fractured tight cores. Besides, the oil distribution of different pore spaces of cores before and after displacement and the main contribution spaces on oil recovery were quantitatively analyzed by using nuclear magnetic resonance and core mercury porosimetry techniques. The results indicate that compared with natural gas flooding, the WANG flooding can retard gas channeling, increase formation energy, and enhance oil recovery by up to 14.1%, especially in fractured cores. Under the resistance of water slugs, the gas was allowed to enter smaller pores and its swept volume was expanded. Oil is mainly stored in mesopores (0.1–1 μm) and small pores (0.01–0.1 μm), accounting for over 90% of the total volume. The oil recovered mainly comes from mesopores, which accounts for over 75% of the total amount. Moreover, the WANG flooding strengthens the recovery of oil in mesopores and macropores (1–10 μm), but it also squeezes oil into small pores and micropores (0.001–0.01 μm).

Keywords NMR · Water-alternating-natural gas flooding · Tight reservoir · Gas channeling · Pore space

List of symbols

a_i	The surrounding area difference of relaxation time range i before and after flooding
A	The surrounding area of the T_2 distribution before flooding
b_i	The surrounding area of the T_2 distribution of relaxation time range i after flooding
B	The area surrounded by the T_2 distribution after gas flooding and the abscissa axis
$c_{i\text{-NGF}}$	The CVFOR within the relaxation time range of i before flooding
$c_{i\text{-WANGF}}$	The CVFOR within the relaxation time range of i after flooding
c_i	The CVFOR within the relaxation time range of i
C	The conversion coefficient
e	The power constant
f_i	The distribution frequency, %
F_S	The pore shape factor
G_i	The growth coefficient of CVFOR within the relaxation time range of i
k_{fi}	The fracture i permeability of the core, mD
k_m	The matrix permeability of the core, mD
k_t	The total permeability of the core, mD
p_i	The volume proportion of pore space of relaxation time range i, %
r_c	The pore radius, μm
r_i	The pore throat radius of distribution frequency i, μm
r_t	The pore throat radius, μm
R	The oil recovery of the tight core, %

✉ Chuanjin Yao
  cy375@upc.edu.cn

1 Key Laboratory of Unconventional Oil and Gas Development, Ministry of Education, China University of Petroleum (East China), Qingdao 266580, People's Republic of China

2 School of Petroleum Engineering, China University of Petroleum (East China), Qingdao 266580, People's Republic of China

3 Research Institute of Petroleum Exploration and Development, PetroChina, Beijing 100083, China

R_{NGF}	The oil recovery of the tight core after gas flooding, %
R_{WANGF}	The oil recovery of the tight core after WANG flooding, %
S	The surface area of rock, μm^2
T_2	The transverse relaxation time of hydrogen atoms, ms
T_{2b}	The relaxation time of hydrogen atoms, ms
T_{2i}	The relaxation time of distribution frequency i
V	The specific surface area, μm^3
α	The average pore-throat ratio of a tight core
θ_i	The angle between fracture i and the direction of fluid flow, °
ρ_2	Is the relaxation surface rate, $\mu m/ms$

Abbreviations

BPR	Back-pressure regulator
CVFOR	Contribution value for oil recovery
HTHP	High temperature and high pressure
MIP	Mercury intrusion porosimetry
NECH	Number of echoes
NMR	Nuclear magnetic resonance
NS	Number of scans
P1, P2	Pulse width
PV	Pore volume
SIRT	Simultaneous iterative reconstruction technique
TE	Echo time
TW	Waiting time
WAG	Water-alternating-gas
WANG	Water-alternating-natural gas

Introduction

The tight oil reservoir is rich in reserves and has a broad development prospect, but it also has the characteristics of low permeability and high development difficulty. At present, tight oil reservoirs are mainly developed by gas injection after fracturing, such as carbon dioxide, nitrogen, and methane (Yang et al. 2013; Zou et al. 2012). Carbon dioxide has been successful, but its insufficient gas source and corrosiveness make it unsuitable for the development of tight reservoirs in China (Song et al. 2020). As oilfield-associated gas, natural gas has attracted wide attention in recent years. Associated gas needs to be removed from the useless gas and transported in the treatment process of oilfields, and its cost is high. However, it is feasible to inject associated gas back into the reservoir. On the one hand, the amount of associated gas is sufficient, which solves the problems of its storage, transportation, disposal, and sale. On the other hand, reinjection does not create compatibility issues on rock or fluid. It is also noncorrosive, which is superior to carbon dioxide. The study shows that natural gas injection in tight reservoirs has a good development effect, so the method is more compatible with tight reservoirs (Jin et al. 2017; Tran et al. 2021).

In tight oil reservoirs, considerable production can be achieved in the early stage of gas injection, but the production decline speed is fast. Volume fracturing can effectively improve the injection ability of fluid in reservoirs, but the existence of fractures also makes the fluid flow along the fracture first (Fernø et al. 2015; Qu et al. 2022). The swept range of injected gas is low, and the gas channeling is serious in tight reservoirs (Lescure and Claridge 1986; Ji et al. 2022). Therefore, slowing down the gas channeling and expanding the swept range of the injected gas is crucial for improving the development effect of tight reservoirs. The water-alternating gas (WAG) flooding is an effective way to retard gas channeling (Christensen et al. 2001; Wang and Locke 1980). Lei et al. (2016) found that CO_2-WAG flooding after continuous CO_2 flooding can observably improve the oil production of the entire reservoir, especially in the heterogeneous reservoir. Christensen et al. (2001) pointed out that water-alternating natural gas (WANG) flooding had the potential to improve micro-displacement efficiency compared to gas flooding and discussed the factors that affect WAG flooding, including rock and gas types, injection plans, and well spacing. Besides, they found that compared to carbon dioxide, natural gas did not cause corrosion issues in injection and production equipment, which was important, especially in offshore environments with limited problem-solving capabilities. Al-Bayati et al. (2018) showed that water slugs of WAG can reduce the relative permeability of gas, thereby reducing the mobility of displacement, thus improving the macroscopic displacement efficiency and the microscopic swept volume of gas. In addition, some studies also concluded that WAG flooding was superior to traditional gas flooding because the gas could flow well between fractures and pores (Ebadati et al. 2018, 2019). Wang et al. (2022) studied the application of WANG and intermittent gas injection in ultra-low permeability reservoirs and found that both can improve oil displacement efficiency. Besides, compared with gas, the injected water has a high viscosity and poor flow ability, which can form resistance in front of the gas slug to make the gas flow around, thus improving the swept volume of the gas. Therefore, studying the water–gas slug ratio is important. The high water–gas slug ratio forms a high flow resistance, which not only leads to slow oil production in the outlet section but also results in a large pressure difference between the injection well and production well and increases the difficulty of on-site operations. The smaller the water–gas slug ratio, the less significant the effect of water, and the worse the effect of improving gas swept volume, and the final oil recovery cannot be significantly improved.

The pore structure of tight reservoirs is complicated. Especially after fracturing, the distribution law of movable crude oil is more complex (Wang et al. 2009; Yang et al. 2007). In recent years, nuclear magnetic resonance (NMR) technology has become an important way to study pore structure and fluid flow in reservoirs, because of its ability to monitor the hydrogen of fluid (Ausbrooks et al. 1999; Huang et al. 2018). The NMR T_2 distribution can be obtained by scanning the saturated oil core, which can be used to describe the distribution of saturated fluid by showing the hydrogen intensity of the fluid at different relaxation times (Huang et al. 2022; Yao and Liu 2012). Large relaxation time represents a large pore radius. However, the T_2 distribution can only reflect the relaxation time, which cannot accurately characterize the actual size of the pore radius. However, the core mercury intrusion porosimetry (MIP) test can accurately get the pore throat size distribution of rock (Hassnizadeh et al. 2002). The pore radius and pore-throat radius also can be converted to each other by the average pore-throat ratio. By combining the core MIP data with NMR data, many scholars established the conversion equation between pore throat radius relaxation time (T_2) and then, transformed T_2 distribution into fluid distribution at different pore throat radii (Lang et al. 2021; Li et al. 2015; Yao et al. 2010). Li et al. (2015) studied the pore structure characteristics of a tight reservoir based on this method and applied the NMR pore throat distribution curve to oilfield development evaluation. Huang et al. (2021) used this method to analyze the movable fluid space distribution in tight reservoirs. In our study, the distribution and recovery characteristics of oil in tight cores, gas channeling prevention mechanisms, and main influence pore spaces of WANG were quantitatively analyzed through the method.

In this paper, the core samples from the X block of Changqing Oilfield in China were selected. The core was made the fracture along the end face for simulating the fracturing features of the actual tight oil reservoirs. A gas flooding experiment and three WANG flooding experiments with different water–gas slug conditions were conducted by high temperature and high-pressure (HTHP) experimental device. The distribution of oil before and after displacement was studied based on the MIP and NMR techniques. The effects of WANG flooding on preventing gas channeling and enhancing oil recovery were studied quantitatively at the pore scale. The evaluation parameters (contribution value for oil recovery) were established to study the influences of WANG flooding on oil distribution in different pore spaces. The paper provides theoretical guidance for the efficient development of tight reservoirs.
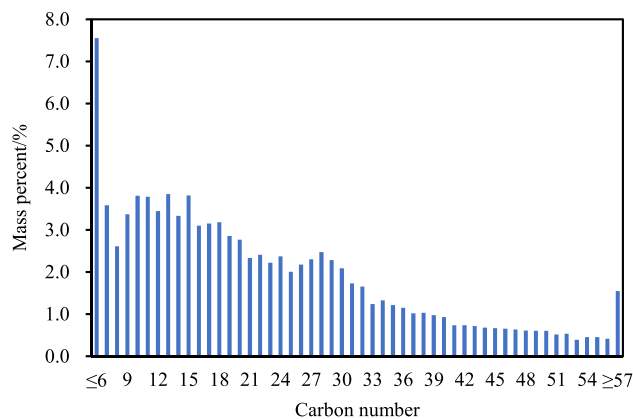

Fig. 1 Carbon distribution of crude oil

Table 1 Composition of the natural gas

Component	CO_2	CH_4	C_2H_6
Mole fraction (mol%)	1.01	77.52	21.47

Experiments and methods

Experimental materials

The experimental oil was made by adding white oil to the degassed oil from the X block of Changqing Oilfield. The aim is to make the viscosity of the experimental oil the same as that of the formation oil under experimental conditions, the viscosity value is 1.8 mPa·s at 70 °C. The reason is that the bubble point pressure is 10.937 MPa under a formation temperature of 70 °C. Under the condition, the experimental pressure is higher than the bubble point pressure, and there is little difference in experimental results between the experimental oil and non-degassed oil. The displacement effect of crude oil mainly depends on the mobility ratio between injecting fluid and saturated oil. The carbon number distribution of degassed oil is shown in Fig. 1, which was tested by using the Agilent 7890A gas chromatography of Agilent Technologies.

The components of natural gas include methane, ethane, and carbon dioxide, which were provided by Huicheng Ruike Company. Based on the associated gas components of the oil production well, the components were re-proportioned, as shown in Table 1.

The experimental water was made up of deionized water and inorganic salts based on the salinity composition and the ion content of the strata water in the oilfield, as shown in Table 2. In addition, the Mn$^+$ was added to the experimental water to make the concentration of Mn^{2+} in the solution reach 15,000 mg/L, so as to shield the hydrogen

Table 2 Composition of strata water salinity

Component	Na$^+$ + K$^+$	Mg^{2+}	Ca^{2+}	Cl$^-$	HCO$_3^-$	SO$_4^{2-}$	Total
Ion concentration (mg/L)	16,207	270	2528	29,703	337	734	53,900

Table 3 Physical properties and fracture conditions of two cores

Core no.	Permeability (mD)	Porosity (%)	Diameter (mm)	Length (mm)
1	0.0378	10.24	25.00	50.24
2	0.0331	9.62	24.50	51.08

Fig. 2 Core samples used in the experiments

of the water and ensure that the hydrogen detected by NMR is the hydrogen in the experimental oil.

The core samples were also cut from the X Block of Changqing Oilfield. Each flooding experiment includes two cores, and the core parameters are shown in Table 3. The measuring method of core permeabilities was the steady-state method by injecting N$_2$. The core permeability values were the average value by multiple measurements. In addition, core No.2 was selected to make the fracture to simulate the actual reservoir fracturing conditions. The fracture length is 51.08 mm, and the fracture width is 1.40 mm. The fracture permeability was measured by the permeability formula of the matrix-fracture system, which was about 68.02 mD. The core samples are shown in Fig. 2. Parsons (1966) divided the permeability of matrix-fracture system cores into two parts to consider, namely matrix permeability and fracture permeability. The permeability of the matrix-fracture system can generally be determined by the superposition of matrix permeability and fracture system permeability. The calculation formula is as follows.

$$k_t = k_m + \sum k_{fi} \cos_{\theta i} \tag{1}$$

where k_t is the total permeability of the core, mD; k_m is the matrix permeability of the core, mD; k_{fi} is the fracture i permeability of the core, mD; θ_i is the angle between fracture i and the direction of fluid flow, °.

Experimental equipment

The experimental equipment of WANG flooding is shown in Fig. 3, which mainly includes natural gas cylinder, booster pump, injection pump, intermediate containers, core holder, manual annular pump, oil–gas separation and collection device, and NMR device. The injection pump is a VP-12 K-T-C high-pressure injection pump provided by Vindum Engineering. The injection pump can monitor the outlet pressure and adjust the injection flow rate in real-time, which can achieve the outlet pressure range of 0–82.7 MPa and fluid injection rate range of 0.00001–30 mL/min. The pressurized gas and water were driven into the core holder by the injection pump. Two intermediate containers were used to store the natural gas and water, separately. The core holder was designed and produced by Lianyou Company (Jiangsu, China), which can withstand the maximum temperature and pressure were 50 MPa and 120 °C, respectively. The core holder was equipped with a temperature-controlled cabinet to control the temperature, and the control precision was 1 °C. Besides, the pipelines between the intermediate container and the core holder were enveloped by the heatproof lagging. A manual annular pump with a range of 0–50 MPa was used to control the annular pressure. The outlet pressure was controlled by a back-pressure regulator (BPR). The pressure range can be set by the BPR is 0–30 MPa. The production oil and water were collected by the measuring cylinder, and the mass of them was corrected by using the balance, and the produced gas was collected by the draining water gathering gas method.

The NMR device is the MacroMR12-150H-VTHP NMR apparatus of Niumag Corporation (Shanghai, China), which was used to obtain the T_2 distribution to analyze the recovery law at the pore scale. The magnetic field intensity of the NMR instrument is 0.25–0.35 T. The type of probe is MacroMR12-150H-I-25 mm. The other settings were as follows: the TW (waiting time) was 2000 ms, the TE (echo time) was 0.075 ms, the NECH (number of echoes) was 18,000, and the NS (number of scans) was 32. The pulse width included two pulse widths, which were set as P1 = 6 (90° pulse width) and P2 = 10.24 (180° pulse width). The relaxation time range of T_2 distribution was 0.01–10000 ms, and the number of data points was 200. In addition, the inversion process was
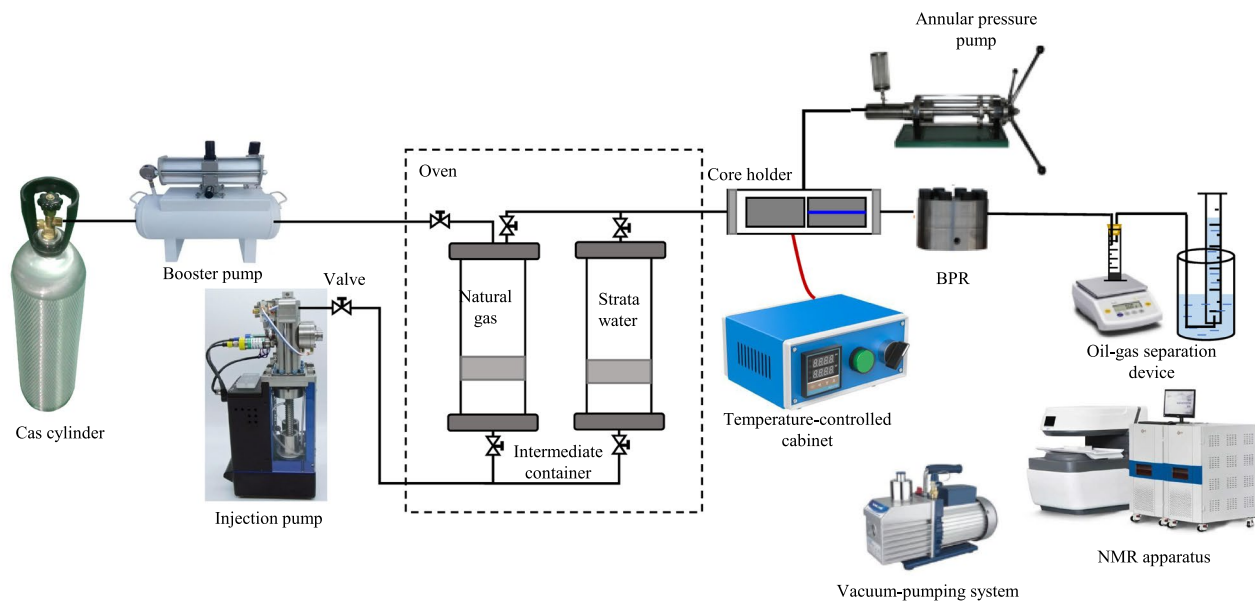
Fig. 3 Flowchart of the WANG flooding experimental device

set as: the selecting method was sampling, the inversion was simultaneous iterative reconstruction technique (SIRT), the filter gear was 3, the iteration number was 10,000 and the component option was multiple components. The NMR tests were conducted offline because the apparatus could not withstand the high experimental temperature and pressure. Many inversions were performed for each NMR test. The NMR apparatus was calibrated before every test.

The position of the two experimental cores is shown in Fig. 3. The fractured core was placed near the outlet of the core holder. The purpose is to accord with the situation of the oilfield. The production well is usually fractured for reducing seepage resistance. But the gas injection well is not fractured for avoiding gas channeling. On the one hand, the injection well can form fractures due to the high pressure of the injected gas. But the pressure of production well is relatively low. On the other hand, fracturing the injection well can lead to gas channeling, while fracturing the production well can promote fluid flow into the bottom hole. Fractures of gas production wells also are helpful to utilize the natural energy in the initial production stage.

Experimental steps

At first, the two experimental cores were cleaned and extracted with CCl_4 solution by using the Soxhlet extractor. If the color of the solution does not change after cleaning, the core cleaning is considered to be finished. And then, the experimental cores were placed in an oven to dry at 70 °C. After that, core No.2 was cut by the core cutter along the vertical direction of the end face. The glue (the epoxy resin adhesive and epoxy curing agent) was uniformly mixed with quartz sand (40–70 mesh) according to the volume ratio of 1:10. The mixture was filled in the cutting fracture to simulate the actual reservoir fracture. Finally, the core was dried in the oven for 12 h at 70 °C. After the fractured experiment, the WANG flooding and natural gas flooding experiments were started. The steps of our experiments are as follows:

(1) Two experimental cores were weighed, vacuumed, and saturated oil, and the saturated oil cores were tested by the NMR apparatus. The saturated oil cores were recorded by weight for calculating porosity and placed in the core holder. The annular pressure and temperature were set as 30 MPa and 70 °C.

(2) The natural gas was pressurized to 20 MPa at room temperature and filled with the intermediate container, which was placed in an oven at 70 °C for 12 h. Because the natural gas was heated to expand, the container pressure started to rise from 20 MPa and reached stability (< 30 MPa).

(3) The deionized water was injected into the pipeline between the core holder and the BPR. The purpose is that when oil flowed out of the core holder, it could displace the water flow in the pipeline. Then, the initial moment of oil production can be observed. The oil production speed also can be calculated according to the flow rate of deionized water.

(4) The injection pump mode was set as constant pressure injection of 26 MPa and the pressures of natural gas and water in intermediates were pressurized to 26 MPa

in advance. The BPR pressure was also adjusted to 16 MPa.

(5) The valve between the natural gas intermediate container and the core holder was opened. The natural gas was injected at a constant flow rate(0.03 mL/min). After 0.17 pore volume (PV) gas was injected, the experimental water and natural gas were injected alternately. The 0.17 PV was the injected gas volume of the first WANG experiments when the deionized water at the outlet of the BPR began to migrate. To maintain consistency in experimental conditions, the 0.17 PV was defined as the gas injection volume at which crude oil begins to be produced. For all WANG experiments, the water was injected after injecting 0.17 PV natural gas.

(6) The volume of the water–gas slug was injected according to the proportion of 1:3, 1:1, and 3:1, respectively. The total volume of every water–gas slug was 0.8 PV. A total of three water–gas slugs were injected in each WANG experiment. For the natural gas experiment, the natural gas was continuously injected until the gas channeling was observed.

(7) The pipeline from the end of the BPR to the measuring cylinder was transparent. When the water flow in this pipeline was observed, the production data were recorded. At this point, the oil in the core has begun to be driven out. The initial oil production rate was determined according to the deionized water production rate.

(8) When the bubbles were found in the gas-collecting device, the gas production data were recorded. The production gas-oil ratio was calculated according to the volume of oil and gas collected over a period of time.

(9) After injecting the fluid (natural gas and deionized water) of 2.57 PV ($2.57 = 0.17 + 0.8 \times 3$), the WANG experiment was stopped and the core was tested by NMR.

Calculation of the relationship between relaxation time of NMR and pore throat radius

The transverse relaxation information of hydrogen in the fluid can be detected by the NMR test, and then, the distribution of oil in different pore spaces can be obtained. The relaxation time T_2.was used to describe the relaxation information of oil. As the hydrogen nucleus relaxes, it collides with the rock pore wall. When the pore radius of rocks is smaller, hydrogen nuclei are more likely to collide, and hydrogen nuclei will suffer energy loss after the collision. Hence, the smaller the pore radius, the greater the relaxation rate of hydrogen nuclei. In a uniform magnetic field, the transverse relaxation time of atoms in the pore could be approximated as Eq. (2) (Fang et al. 2017; Wang et al. 2010):

$$\frac{1}{T_2} = \frac{1}{T_{2b}} + \rho_2 \frac{S}{V} \tag{2}$$

where T_{2b} is the relaxation time of hydrogen atoms, ms; ρ_2 is the relaxation surface rate, μm/ms, which is mainly determined by the properties of core (mineral composition, etc.) and fluid; S/V is the specific surface area, $μm^2/μm^3$.

The value of T_{2b} is usually much greater than T_2, so the first term after the equal sign can usually be omitted:

$$\frac{1}{T_2} = \rho_2 \frac{S}{V} \tag{3}$$

When the pore structure of tight cores is simplified to spherical and cylindrical, the relationship between pore radius and specific surface area can be established by introducing a factor:

$$\frac{S}{V} = \frac{F_S}{r_c} \tag{4}$$

where r_c is the pore radius, μm; F_S is the pore shape factor.

Further, we can get the relationship between the T_2 and pore radius can be gotten, as shown in Eq. (5). However, the pore structure of rock in the actual tight reservoir is complicated. A large number of test results that the T_2 and pore radius have a power function relationship (Li et al. 2015). In addition, for the same core, the correlativity between the pore throat radius and pore radius is shown in Eq. (7).

$$T_2 = \frac{r_c}{\rho_2 F_S} \tag{5}$$

$$T_2 = \frac{r_c^e}{\rho_2 F_S} \tag{6}$$

$$r_c = \alpha r_t \tag{7}$$

where r_t is the pore throat radius, μm; α is the average pore-throat ratio of a tight core; e is the power constant.

The α, ρ_2, and F_s are constant for a core saturated fluid. By further introducing the conversion coefficient C, the pore throat radius of the tight core can be described by the T_2 value:

$$C = \frac{\left(\rho_2 F_S\right)^{1/e}}{\alpha} \tag{8}$$

$$r_t = C T_2^{1/e} \tag{9}$$

The pore throat size and pore space distribution frequency can be obtained by the MIP curve. According to

the MIP and NMR testing data of the same core, the constants C and e in Eq. (9) can be obtained.

Figure 4 shows the T_2 spectra of a core before and after natural gas flooding; the T_2 spectrum area after gas flooding is obviously smaller than that before gas flooding. The pore volume proportion of different relaxation time ranges can be calculated according to the surrounding area of the curve, as shown in Eq. (10) (Wang et al. 2020; Gao et al. 2021). The original saturated oil volume in the pore space of i is $a_i + b_i$ and the residual oil volume is b_i.

$$p_i = \frac{a_i + b_i}{A} \tag{10}$$

where p_i is the volume proportion of pore space of relaxation time range i; a_i is the surrounding area difference of relaxation time range i before and after flooding; b_i is the surrounding area of the T_2 distribution of relaxation time range i after flooding; A is the surrounding area of the T_2 distribution before flooding.

Generally speaking, for the same tight core, the oil recovery of large pores is higher than that of small pores. However, the volume of large pores may be limited, which leads to a low contribution to the oil recovery. Therefore, in order to quantitatively study the oil recovery characteristics and the mechanism of gas channeling prevention in the pore scale, the contribution value for oil recovery (CVFOR) of

different pore spaces was introduced as shown in Eq. (11) (Yao et al. 2022). This calculation method is based on T_2 data before and after flooding and the oil recovery. The sum of all CVFOR of different pore spaces is the total core oil recovery. The value cannot only describe the recovery effect of oil in different pore spaces but also can be used to analyze the influence degree of WANG on retarding gas channeling for the oil in different pore spaces. In addition, the index of the growth coefficient of CVFOR was introduced to evaluate the effect of WANG on CVFOR in different space pores.

$$c_i = \frac{a_i}{A - B} \times R \tag{11}$$

$$G_i = \frac{c_{i-\text{WANGF}} - c_{i-\text{NGF}}}{R_{\text{WANGF}} - R_{\text{NGF}}} \times 100\% \tag{12}$$

where c_i is the CVFOR within the relaxation time range of i; B is the area surrounded by the T_2 distribution after gas flooding and the abscissa axis; R is the oil recovery of the tight core, %; G_i is the growth coefficient of CVFOR within the relaxation time range of i; $c_{i-\text{WANGF}}$ is the CVFOR within the relaxation time range of i after flooding; $c_{i-\text{NGF}}$ is the CVFOR within the relaxation time range of i before flooding; R_{NGF} is the oil recovery of the tight core after gas flooding, %; R_{WANGF} is the oil recovery of the tight core after WANG flooding, %.

Results and discussion

The conversion relationship of the relaxation time and pore throat radius

The core with a permeability of 0.0344 mD was selected to calibrate the relationship between relaxation time and pore throat radius, which came from the same long core as the experimental core. The T_2 distribution of the core is shown in Fig. 5a. There are two obvious peaks in the distribution, which indicates that the pore space corresponding to these two relaxation times contains more oil. In addition, the oil
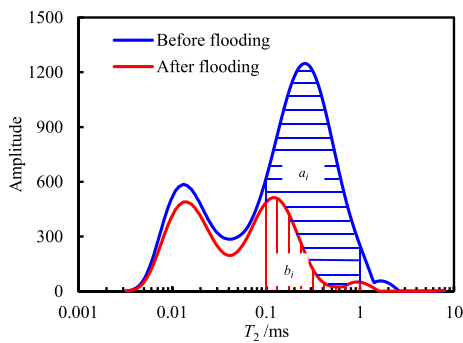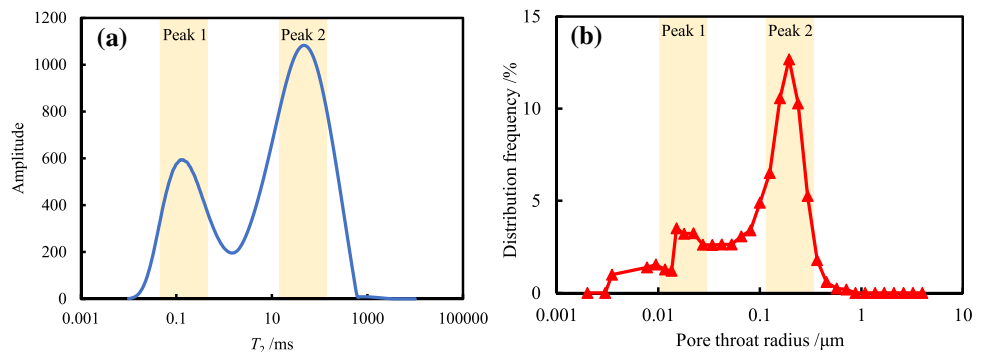

Fig. 4 Calculation diagram of the proportion of pore space

Fig. 5 NMR and MIP result of a tight core: **a** T_2 spectrum; **b** pore throat radius distribution curve

is mainly stored in the pore space with a relaxation time between 0.01 and 1000 ms. The capillary pressure data also were obtained by the core MIP test. The distribution frequency curve of the pore throat radius is further drawn, as shown in Fig. 5b. The pore throat radius distribution curve is similar to the T_2 distribution curve in shape. The pore throat radius distribution curve also has two obvious peaks at pore throat radius of 0.018 and 0.19 μm.

The pore throat radius cumulative distribution frequency curve and the T_2 cumulative distribution frequency curve of the same tight core were drawn in the same logarithmic coordinate system (Fig. 6). The results show that the two curves have a high degree of matching. In the blue-shaded area, each distribution frequency f_i corresponds to a relaxation time (T_{2i}) and a pore throat radius (r_i), as shown in the green line of Fig. 6.

Many cumulative distribution frequency points were selected in the taking value interval. The frequency points were drawn in a double logarithmic graph with the relaxation time T_{2i} as the abscissa value and the pore throat radius r_i as the ordinate value (Fig. 7). Further, the data points were fitted into a straight line; thus, the relationship between the relaxation time and the pore throat radius was obtained, as shown in Eq. (13). The fitting degree of the curve is 97.89%, and the fitting degree is good.

$$r_t = 0.0491 T_2^{1/1.8155} \tag{13}$$

The transformed distribution is shown in Fig. 8; it can be found that the oil is mainly distributed in the spaces of 0.01–1 μm pore throat radius. On this basis, in order to quantitatively research the recovery characteristics of oil in different pore spaces and evaluate the effect of WANG to retard gas channeling, the pore spaces of cores are divided into four types: micropores, small pores, mesopores, and macropores. The range of pore space applies only to this

paper. The relaxation time range and pore throat radius range are shown in Table 4.

Effect analysis of enhancing oil recovery and preventing gas channeling by WANG flooding

Natural gas flooding experiment

In order to compare the effect of WANG flooding on retarding gas channeling and enhancing oil recovery, the natural gas flooding experiment was conducted first. As shown in Fig. 9, the injection pressure, oil recovery, and production gas-oil ratio varied with the gas injection volume. The production gas-oil ratio data were calculated in the laboratory environment (atmospheric pressure and room temperature). It could be found that the injection pressure decreased continuously with the injection of natural gas. The result indicates that the gas flooding cannot maintain the pore pressure of the core, and it is difficult to replenish the formation energy. The fluid can flow smoothly in the experimental core with the injection-production pressure difference. Besides,
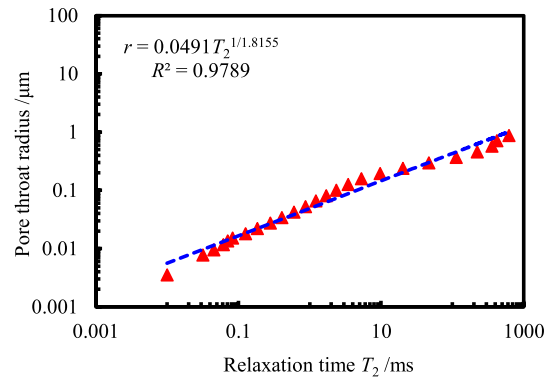

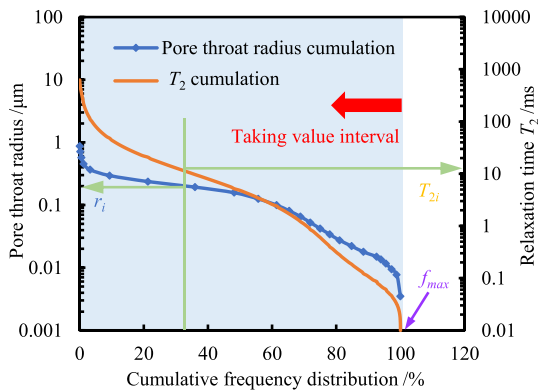
Fig. 7 Numerical fitting curve

Fig. 6 Cumulative distribution frequency curve of relaxation time and pore throat radius
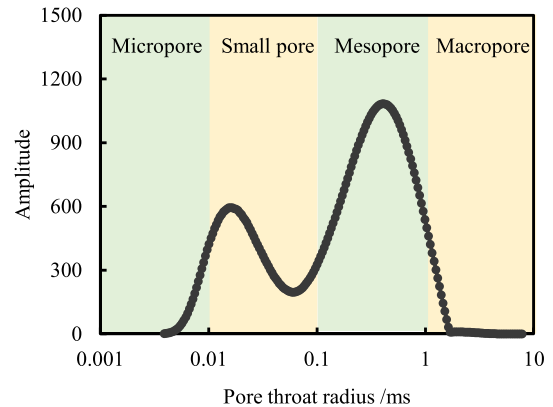

Fig. 8 Transformed T_2 spectrum and the range of different pore spaces

the gas injection rate couldn't make up for the fluid production rate under the pressure difference. This is the reason why the injection pressure decreased continuously. In addition, the pressure decay rate changed from slow to fast, and there was an obvious turning point in the pressure curve when the gas injection volume was about 0.13 PV. The reason was that oil began to be produced at this time. With the production of oil, a fluid flow channel was formed in the core. As shown in the oil recovery variation curve, the oil began to be produced from the core holder when the gas injection was 0.145 PV. Because the produced oil first accumulated in the pipeline, the injection volume point of the oil recovery curve lagged behind the pressure curve. After the oil breakthrough, the fluid flow resistance dropped and the

injection pressure dropped at a greater rate. With the continuous injection of natural gas, saturated oil was produced continuously. After the oil breakthrough for a while, natural gas started to be produced and the production gas-oil ratio increased rapidly. Then, the gas channeling occurred, the oil recovery began to be stable, and the final oil recovery was 38.0%.

WANG flooding experiments.

After that, three WANG flooding experiments with different water–gas slug ratios were also conducted. The variation curves of oil recovery were shown in Fig. 10. For three experiments, the oil recovery increased with the injection

Table 4 Range of different pore spaces of experimental cores

Type of pore spaces	Micropore	Small pore	Mesopore	Macropore
Pore throat radius (µm)	0.001–0.01	0.01–0.10	0.10–1.00	1.00–10.0
T_2 (ms)	< 0.0556	0.056–3.64	3.64–237.90	> 237.90

(a) Variation curve of pressure with injection volume

(b) Variation curves of oil recovery and production gas-oil ratio with injection volume
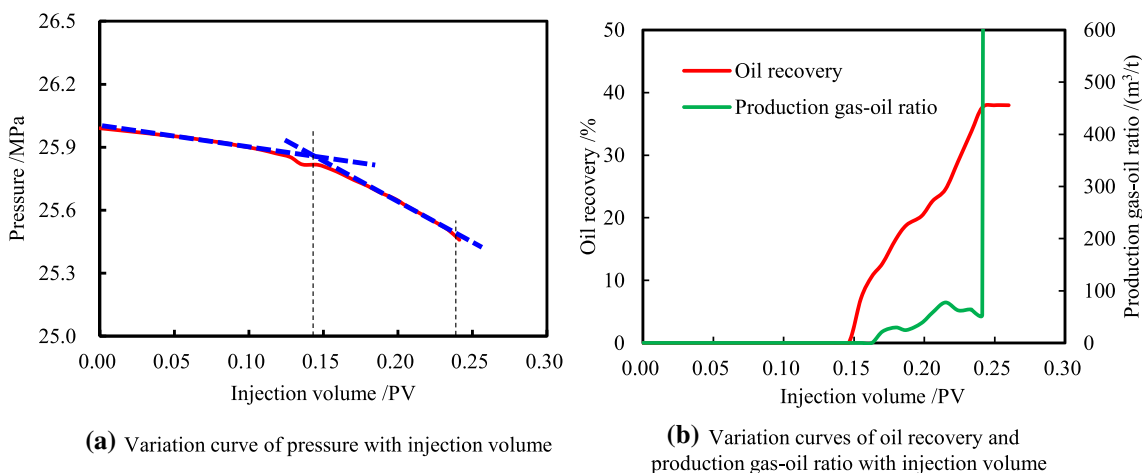
Fig. 9 The gas flooding experimental result

(a) Water-gas slug ratio is 3:1

(b) Water-gas slug ratio is 1:1

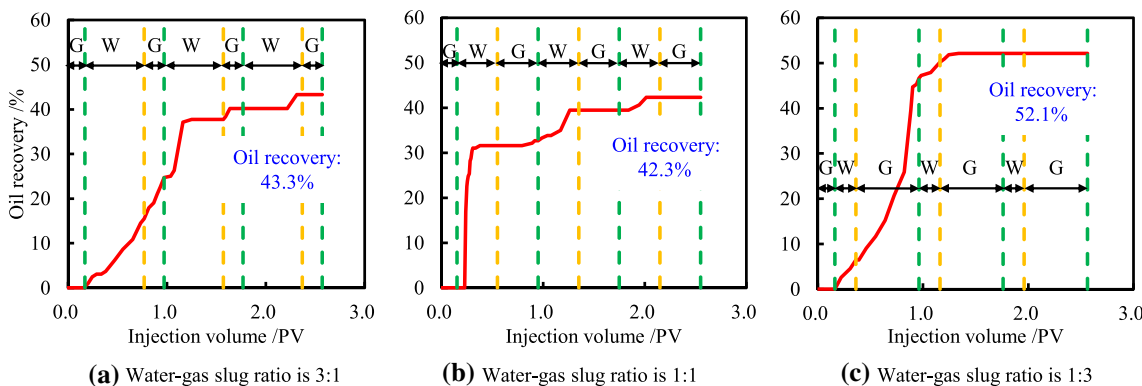**(c)** Water-gas slug ratio is 1:3

Fig. 10 Variation curves of oil recovery of WANG flooding experiments with different water–gas slug ratios

of fluid. And the curves all performed that the oil recovery increased rapidly in the early stage and increased in a multi-stage form at the later stage. The reason is that with the injection of fluids, a pressure difference forms between the two ends of the core, and the injected fluid replaces the saturated crude oil. Therefore, the oil recovery can rapidly and steadily increase in the early stage of flooding. After that, as the water was injected, the resistance of gas flow in the rock core increased, and the gas began to flow in all directions and enter smaller pores. At the end of the core, there was a brief period of no oil, and as the fluid was further injected, the pressure difference before and after the core further increased, which could overcome greater start-up pressure and interface resistance, and allowed more oil to start flowing, especially in larger pores. This also led to more crude oil being trapped in small pores. Therefore, the multi-stage form is mainly due to the discontinuity of oil production caused by the water slug. Besides, with the proportion of the water slug decreasing, the faster the oil recovery reached the maximum, the faster the overall oil recovery rate. The reason was that the oil was mainly carried by natural gas, and the existence produced by the water slug led to the gas slug cannot continuously flow. The existence of water slowed the flow of natural gas and oil, and the influence increased with the volume of water. In addition, compared with gas flooding, three WANG flooding experiments improved the oil recovery. When the water–gas slug ratio was 1:3, the oil recovery increased by 14.1%. The results also show that the oil recovery does not increase with the increase of water slug volume. On account of the low permeability of the tight cores and the high flow resistance of water, a small amount of water can effectively improve oil recovery. Although the presence of the water slug can delay the natural gas channeling and increase the swept volume of injecting gas, the increase of water slug volume also produces the flow resistance to affect the flow of natural gas and oil, thus affecting the oil recovery. Therefore, the appropriate amount of water should be chosen for WANG flooding.

The curves of the production gas-oil ratio with gas injection volume of three WANG experiments were shown in Fig. 11. Compared with the result of natural gas flooding, the WANG flooding can effectively retard gas channeling and reduce the production gas-oil ratio. This is because the presence of water slugs can increase the resistance of gas flow. Under the influence of water slugs, gas cannot quickly flow through the core along the main channel, but instead flows around, the swept volume of gas also increased. And as the pressure increases, on the one hand, gas diffused more into the crude oil, and on the other hand, gas overcame the capillary force and entered smaller pores. Therefore, the production gas-oil ratio significantly decreased. The results also demonstrate that the overall production gas-oil ratio in the experimental process increases with the decrease of water slug volume. When the water–gas slug ratio is 3:1, only a higher value occurred when the first gas injection slug broke through. This is because most of the injected gas was trapped in the cores. With the injection of the water slug, only a small amount of gas was produced and the gas-oil ratio was close to 0 m^3/t in the later stage. Under this water–gas slug ratio, the gas injection volume is less and no gas channeling occurs. The result indicates that a lot of water prevents the gas from flowing out along the fracture and the gas may be squeezed into the smaller pores of the matrix. When the water–gas slug ratio is 1:1, the production gas-oil ratio value fluctuates violently, but it never exceeds the 1200 m^3/t. The result means that gas can periodically flow out of the fracture, and the water slug can still effectively inhibit gas channeling. For the experiment with a water–gas slug ratio of 1:3, the production gas-oil ratio increased jumpily. When the injection volume is 1.5 PV, the gas-oil ratio exceeded 5000 m^3/t. The reason for the high gas-oil ratio is that oil production is low at this time, and gas production is much more than oil production. By comparing Figs. 9b, 11c, it can be found that the gas breakthrough time is obviously delayed, and the gas channeling phenomenon is alleviated to a certain extent. The results also demonstrate that the increase of
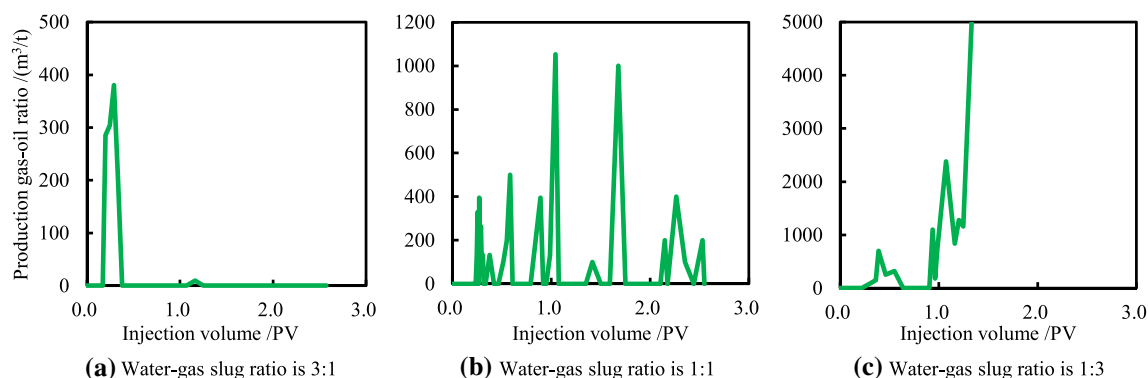

Fig. 11 Variation curves of production gas-oil ratio of WANG flooding experiments with different water–gas slug ratios

(a) Water-gas slug ratio is 3:1 (b) Water-gas slug ratio is 1:1 (c) Water-gas slug ratio is 1:3

(a) Water-gas slug ratio is 3:1   **(b)** Water-gas slug ratio is 1:1   **(c)** Water-gas slug ratio is 1:3
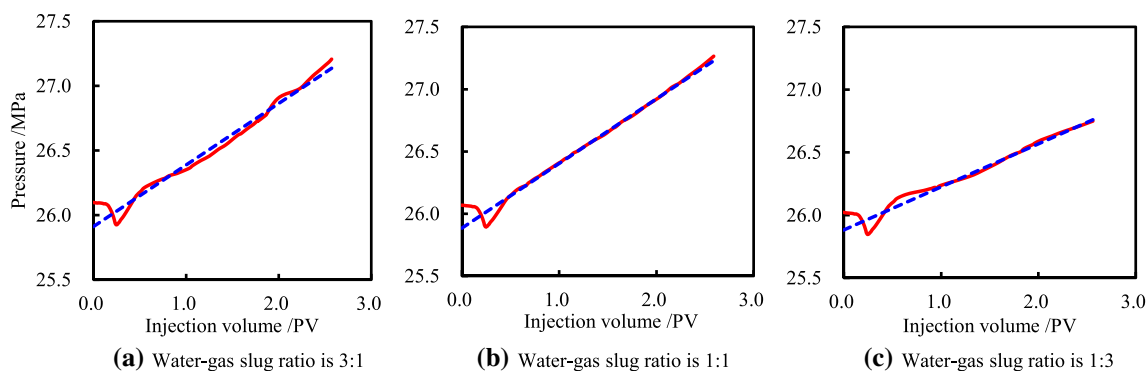
Fig. 12 Variation curves of pressure of WANG flooding experiments with different water–gas slug ratios

water slug volume can effectively prevent gas channeling. In fact, under the resistance of the water slug, part of the injected gas was squeezed into smaller pores which results in less gas production. This conclusion was confirmed in the follow-up of this paper.

The injection pressure of three pressure curves (Fig. 12) all decreases slowly and then, rapidly in the early stage of displacement, which is consistent with the gas flooding experiment. However, after the injection of the water slug, the pressure began to rise under the resistance of injecting water. This demonstrates that the presence of water slugs can significantly increase fluid flow resistance, which leads to a greater pressure difference. This also indicates that the WANG flooding can effectively maintain formation pressure and increase formation energy. It could be found that even if the gas slug was injected later, the pressure curve did not show a downward trend. The reason is that water injection had greater resistance than natural gas injection, and the water could not flow smoothly in this injection speed and pressure difference. In addition, when the water–gas slug ratio is 1:3, the rising speed of pressure is obviously slower than that of the other two experiments. The increase of water slug volume increases the difficulty of injection. All results demonstrated that compared with natural gas flooding, the WANG flooding can effectively improve oil recovery, replenishes formation energy, and alleviate gas channeling.

Mechanism analysis of enhancing oil recovery and preventing gas channeling by WANG flooding at the pore scale

The distribution of oil and the range of movable fluid determine the final production from a tight oil reservoir. The core NMR results (whole group cores) after and before flooding experiments under different conditions were shown in Fig. 13. The black line in Fig. 13 is the result of the initial saturated oil core, and it indicates that the oil is mainly found in small pores and mesopores. The area surrounded
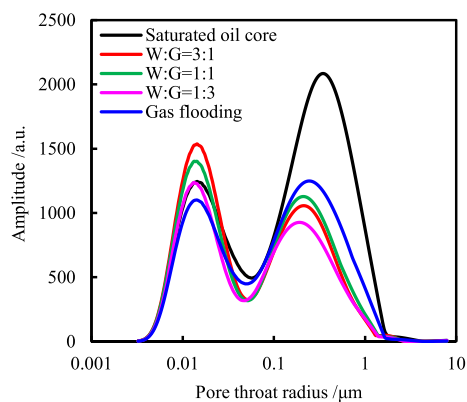

Fig. 13 Core NMR results after and before flooding experiments under different conditions

by the black line and the other colored lines is the distribution of the oil that has been recovered. The blue curve is the experimental result of natural gas flooding, and the results show that the oil in different spaces can be recovered by gas flooding. The gas flooding primarily recovered the oil stored in mesopores, followed by small pores, and less in micropores and macropores. The pore throat radius of mesopores is relatively large, and the capillary force on the oil inside the mesopores is greater than that of the small pores. Therefore, even if there is a large amount of oil in the small pores, its oil recovery is lower than that of the mesopores. Besides, the pore throat radius of the micropores is smaller, the injected gas needs a larger displacement pressure to enter the micropores, and the resistance of the gas carrying the oil out is also greater, so the oil in the micropores is difficult to be recovered. For oil in macropores, although its capillary force is small, on the one hand, the pore space of the macropores is limited, and less oil is stored in the macropores. On the other hand, some oil is adsorbed on the pore wall, so the oil in the macropores cannot be completely displaced. In addition, the recovery of oil in mesopores and macropores was obviously increased by WANG flooding.

Water slugs increase the pressure of the fluid, making it easier for gas to enter the pores, carrying and displacing more oil, and improving oil washing efficiency. At the same time, water slugs effectively alleviate gas channeling, and gas not only flows along fractures but also effectively improves the swept volume of gas. However, the curve results also show that the distribution of oil in small pores and micropores is increased by WANG flooding, which is coincident with our previous analysis. With the resistance of the water slug, the gas flowed in all directions and drove the oil into the smaller space, but this oil was difficult to be displaced due to the large capillary force. It is also found that when the water–gas slug volume ratio is 3:1, more oil was driven into micropores and small pores. This reason was that the greater flow resistance was formed by more water. Although oil was driven into smaller pores by WANG flooding, the presence of a water slug improved the swept volume of the injected fluids. For this reason, the oil distributed in macropores and mesopores was recovered more efficiently, thus improving the oil recovery of the cores.

The volume proportions of different pore spaces were calculated by using Eq. (10) according to the NMR results of the core saturated oil. The results are shown in Fig. 14, which show that the volume proportion of mesopores is the highest, accounting for 59.61%, followed by small pores. Besides, the volume proportion of macropores is the least, on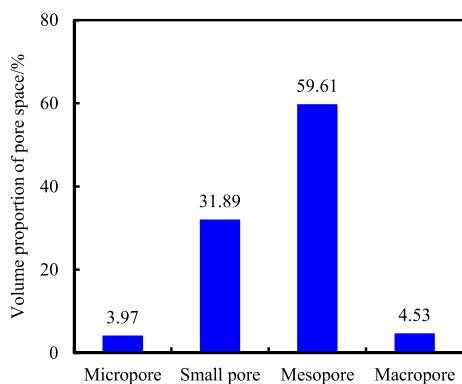ly 4.53%. In addition, the contribution values for oil recovery (CVFOR) of different pore spaces were calculated and the results were also shown in Table 5 and Fig. 15. For natural gas flooding and WANG flooding, the oil in mesopores has a higher CVFOR, mesopores is the main contribution spaces of oil. The recovery of oil in mesopores and macropores was improved by WANG flooding compared with gas flooding. But the CVFOR of oil in micropores by WANG flooding is worse than that of gas flooding. The CVFOR of micropores is negative, which indicates that the oil in micropores increases after the WANG flooding. It is not conducive to developing the oil in micropores by WANG flooding. As the water slug ratio increases, the oil in micropores is more difficult to recover. Although the pore space volume of macropores is much smaller than that of small pores, its CVFOR is close to the CVFOR of small pores, mainly because the oil in macropores is more easily recovered and its oil recovery is higher. For WANG flooding, when the water–gas slug ratio is 3:1, the development of oil in all kinds of pore space shows the best results. In a word, the WANG flooding is an effective method to retard the gas channeling, increase swept volume and enhance oil recovery for tight reservoirs with serious gas channeling or developed fractures.

To further research the recovery oil characteristics and gas channeling prevention mechanism in different cores by WANG flooding, the NMR distributions of two cores in

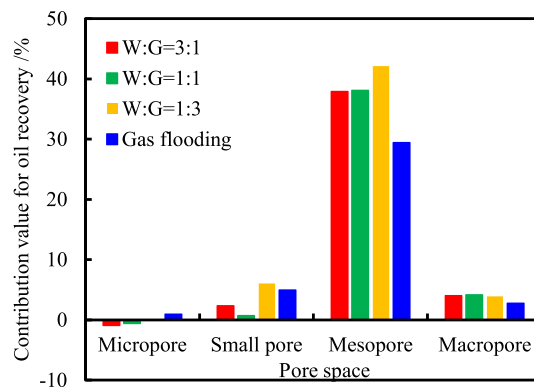Fig. 14 Volume proportion of different pore spaces

Fig. 15 CVFOR of different pore spaces by natural gas flooding and WANG flooding

Table 5 Contribution value for oil recovery and space proportion of different pore spaces

Pore space type	Contribution value for oil recovery			
	Gas flooding (%)	WANG (W:G = 3:1) (%)	WANG (W:G = 1:1) (%)	WANG (W:G = 1:3) (%)
Micropore	0.92	− 0.91	− 0.57	− 0.01
Small pore	4.93	2.33	0.66	6.05
Mesopore	29.41	37.88	38.09	42.14
Macropore	2.74	3.99	4.11	3.92

each experiment were shown in Fig. 16. The results demonstrated that the oil recovered was mainly provided by the non-fracture core, and the phenomenon of the oil displaced into smaller pores mainly appeared in the non-fracture core. Compared with gas flooding, the WANG flooding can effectively recover the saturated oil in four pore spaces of the fractured core. Figure 16a was the distribution of the non-fracture core, the phenomenon was obvious for WANG experiments that the saturated oil was driven into micropores and small pores, especially for the experiment where the water–gas slug ratio was 3:1. In addition, the right end peak value of each WANG flooding experiments' distributions moved to the left, which indicated that the pore throat radius of the saturated oil space became smaller as a whole. When the water–gas slug ratio was 1:3, the oil in mesopores and macropores had the best development effect. As the volume of the water slug increased, more oil was displaced into the small pores and micropores. The T_2 spectra of the fractured core by WANG flooding were shown in Fig. 16b, which illustrated that the recovering oil effects of different pore spaces were much lower than that in the non-fracture core.

Due to the existence of fracture, it was not obvious that oil was driven into smaller pores. However, the oil recovery of different pore spaces was improved by WANG flooding because of the existence of water slug, especially when the water–gas slug ratio is 1:3. The result shows that the existence of water slug can effectually improve the swept volume of fluid and enhance the oil recovery of the fractured core. In summary, the gas channeling was prevented by changing the injected fluid path in the fractured core so that the fluid can flow into smaller pores rather than rapidly along the fracture.

Furthermore, based on the NMR data of two cores under different experimental conditions, the CVFOR of different pore spaces was also calculated by using Eq. (10). The data were shown in Table 6, and the data comparison figure of the two cores is shown in Fig. 17. The data indicate that the oil recovered is mostly come from the non-fracture core, and the CVFOR of the non-fracture core can reach more than 30%. But the total CVFOR of fractured core in gas flooding experiments is even negative, which indicates that the injecting gas preferentially flows along the fracture and cannot recover the oil stored in the matrix. On the other
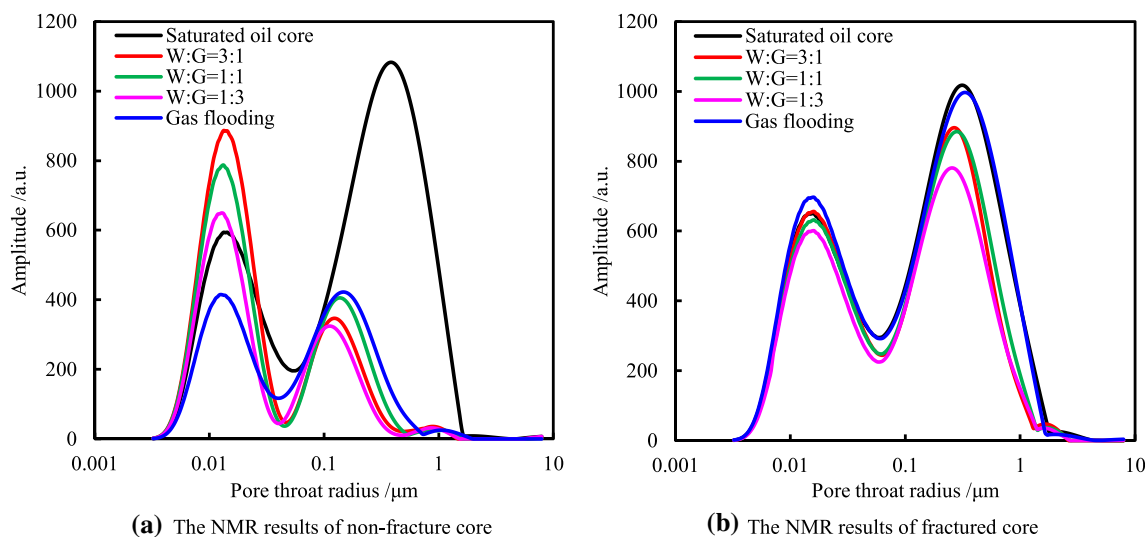

(a) The NMR results of non-fracture core

(b) The NMR results of fractured core

Fig. 16 NMR results of two cores under different conditions

Table 6 CVFOR of different pore spaces of two cores

Pore space type	Gas flooding		WANG (W:G = 3:1)		WANG (W:G = 1:1)		WANG (W:G = 1:3)	
	Non-fracture core (%)	Fractured core (%)	Non-fracture core (%)	Fractured core (%)	Non-fracture core (%)	Fractured core (%)	Non-fracture core (%)	Fractured core (%)
Micropore	1.14	− 0.21	− 1.57	0.16	− 1.22	0.34	− 0.54	0.52
Small pore	5.87	− 0.94	− 1.86	0.88	0.99	1.29	3.44	2.61
Mesopore	29.13	0.28	33.19	8.30	30.20	6.80	31.91	10.23
Macropore	2.35	0.40	2.45	1.76	2.34	1.56	2.27	1.65
Total	38.48	− 0.48	32.21	11.09	32.30	10.00	37.09	15.01

(a) CVFOR of different pore spaces in non-fracture core

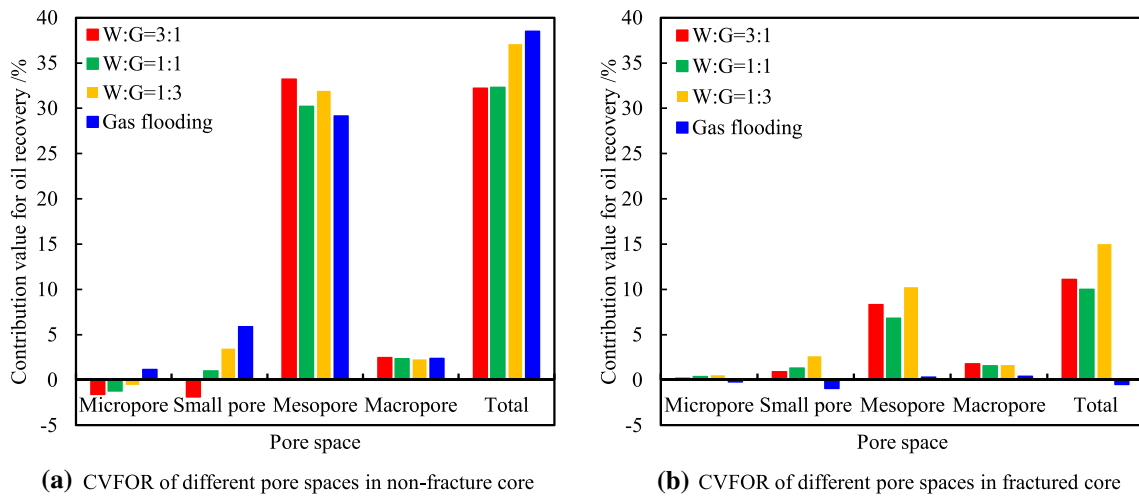(b) CVFOR of different pore spaces in fractured core

Fig. 17 CVFOR of different pore spaces in two cores

hand, as gas migrated and accumulated in the fracture, some of the oil was squeezed and trapped in the smaller pores of the fracture and matrix of the fractured core. However, the CVFOR of the fractured core can be effectively improved by WANG flooding with the influence of water slug. For the non-fracture core, the WANG flooding mainly increases the CVFOR of mesopores, but also leads to the decrease of micropores and small pores, or even negative. The reason is that the amount of oil in these spaces has increased. Besides, the total CVFOR of the non-fracture core by WANG flooding is smaller than the core by natural gas flooding, and the difference is the least when the water–gas slug ratio is 3:1. This suggests that WANG flooding is not a good option in an unfractured tight reservoir. For the fractured core, the CVFOR of natural gas flooding is poor in different pore spaces, but the WANG flooding improves the CVFOR in all four kinds of pore spaces. As the gas slug proportion increases, the CVFOR of micropores and small pores increases, while that of macropores decreases slightly. The experiment with a water–gas slug ratio of 1:3 is still the most effective experiment.

In addition, according to CVFOR values of different pore spaces, the growth coefficients of WANG flooding relative to gas flooding were calculated (Fig. 18). A larger growth coefficient value of the pore space indicates that the WANG flooding has the greatest effect on the CVFOR of this pore space. The results show that WANG flooding mainly influences macropores and mesopores to improve CVFOR, and the growth coefficient of mesopores can reach 200%. Therefore, for tight reservoirs with mesopores development, the WANG flooding is an excellent development method. However, the CVFOR reduction mainly affects the oil in small pores and micropores. Therefore, compared with natural gas flooding, the WANG flooding
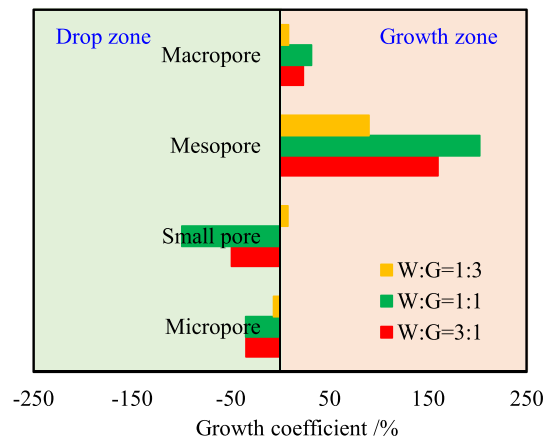

Fig. 18 Growth coefficients of different pore spaces for three WANG flooding experiments

may not be suitable for tight oil reservoirs which widely develop pore spaces with pore radius of less than 1 μm.

The growth coefficients of the two cores were also calculated (Fig. 19). Since the total CVFOR of the non-fracture cores decreases, the negative growth coefficients represent the increase of CVFOR. The results show that the growth coefficient of the non-fracture core is larger and shows a similar law with the whole group of cores. The WANG flooding increases CVFOR of four kinds of pore spaces in fractured cores, especially the mesopore and small pore. Compared with natural gas flooding, the WANG flooding mainly enhances oil recovery and retards gas channeling by changing oil flow in mesopores and small pores.
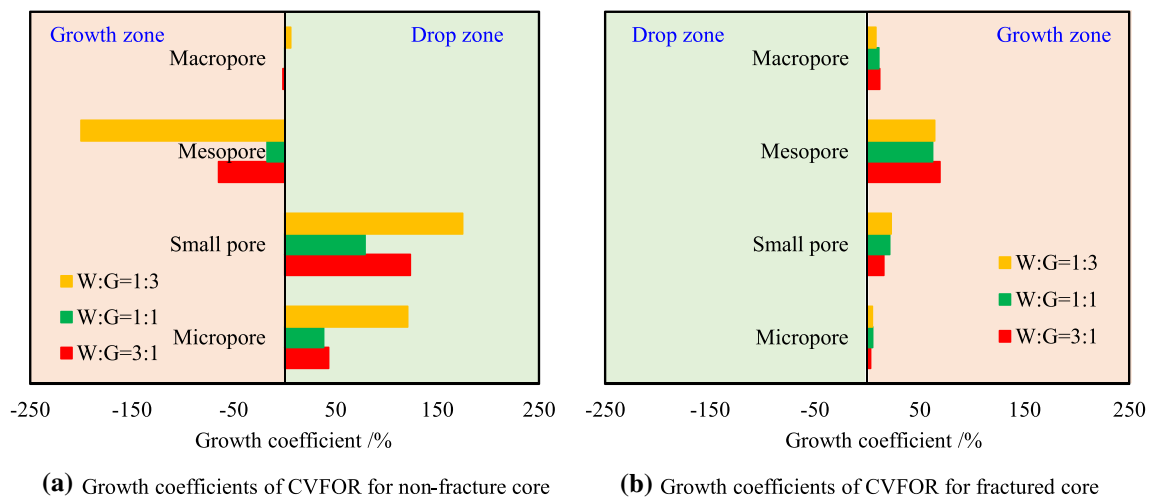
(a) Growth coefficients of CVFOR for non-fracture core

(b) Growth coefficients of CVFOR for fractured core

Fig. 19 Growth coefficients of CVFOR in different pore spaces for two cores

Conclusions

The water-alternation-natural gas (WANG) flooding experiments with different water–gas slug ratios and a gas flooding experiment were conducted by the high-temperature and high-pressure experimental device. The relationship equation between pore throat radius and T_2 was derived, and the T_2 spectra before and after displacement were analyzed by the nuclear magnetic resonance (NMR) technique. Based on the contribution value for oil recovery (CVFOR) and its growth coefficient, the mechanisms of enhancing oil recovery and preventing gas channeling by WANG flooding were quantitatively analyzed at the pore scale. The main conclusions include the following:

1. Compared with natural gas flooding, the WANG flooding can increase injection pressure, retard the gas channeling, enlarge the swept volume of injected gas and enhance oil recovery in tight cores, especially in the fractured core.
2. Due to the flow resistance of water, as the water slug proportion increases, the gas channeling degree becomes lower, but the oil recovery decreases. A small amount of water can greatly enlarge the gas swept volume and increase the oil recovery.
3. The oil recovered by the two flooding methods is mainly from the non-fracture core. For natural gas flooding, the oil recovery of the fractured core is small, and the gas flows preferentially along the fracture. Compared with natural gas flooding, the WANG flooding mainly enhances oil recovery by increasing the swept volume of the injected gas in the fractured core.
4. The volume proportion of mesopores (0.1–1 µm) in tight cores is as high as 58.52%. The oil recovered is

mainly from mesopores and small pores (0.01–0.1 µm). Compared with gas flooding, the WANG flooding can increase the recovery of oil in mesopores and macropores (1–10 µm), but it also squeezes more oil into micropores (0.001–0.01 µm) and small pores, which mainly occurs in the non-fracture core.

5. The WANG flooding mainly affects the distribution of oil in mesopores to improve oil recovery, which increases the CVFOR of mesopores and macropores and decreases the CVFOR of micropores and small pores. The WANG flooding is a good method to develop tight reservoirs with mesopores development after fracturing, but it is not suitable for unfractured reservoirs with smaller pores.

Declarations

Conflict of interest The authors declare no competing financial interest.

References

Al-Bayati D, Saeedi A, Myers M, White C, Xie Q, Clennell B (2018) Insight investigation of miscible $SCCO_2$ Water Alternating Gas (WAG) injection performance in heterogeneous sandstone reservoirs. J CO2 Util 28:255–263. https://doi.org/10.1016/j.jcou.2018.10.010

Ausbrooks R, Hurley NF, May A, Neese D G (1999) Pore-size distributions in vuggy carbonates from core images, NMR, and capillary pressure. In: SPE annual technical conference and exhibition, Houston, Texas, 3–6 October. https://doi.org/10.2118/56506-MS

Christensen JR, Stenby EH, Skauge A (2001) Review of WAG field experience. SPE Reserv Eval Eng 4(2):97–106. https://doi.org/10.2118/71203-PA

Ebadati A, Davarpanah A, Mirshekari B (2018) Stimulated-based characterization recovery enhancement feedback of oil-rim reservoirs. Eng Source Part A 40(21):2528–2541. https://doi.org/10.1080/15567036.2018.1503759

Ebadati A, Akbari E, Davarpanah A (2019) An experimental study of alternative hot water alternating gas injection in a fractured model. Eng Explor Exploit 37(3):945–959. https://doi.org/10.1177/0144598718815247

Fang T, Zhang LK, Liu NG, Zhang LQ, Wang WM, Yu L, Li C, Lei YH (2017) Quantitative characterization of pore structure of tight gas sandstone reservoirs by NMR T_2 spectrum technology: a case study of Carboniferous-Permian tight sandstone reservoir in Linqing depression. Acta Pet Sin 38(8):902–915. https://doi.org/10.7623/syxb201708005

Fernø MA, Steinsbø M, Eide Ø, Ahmed A, Ahmed K, Graue A (2015) Parametric study of oil recovery during CO_2 injections in fractured chalk: influence of fracture permeability, diffusion length and water saturation. J Nat Gas Sci Eng 27:1063–1073. https://doi.org/10.1016/j.jngse.2015.09.052

Gao Y, Li Q, He XM, Yu HT, Wang Y (2021) Quantitative evaluation of shale-oil recovery during CO_2 huff-n-puff at different pore scales. Energy Fuels 35(20):16607–16616. https://doi.org/10.1021/acs.energyfuels.1c02734

Hassnizadeh SM, Celia MA, Dahle HK (2002) Dynamic effect in the capillary pressure-saturation relationship and its impacts on unsaturated flow. Vadose Zone J 1(1):38–57. https://doi.org/10.2113/1.1.38

Huang S, Wu Y, Meng X, Liu LW, Ji W (2018) Recent advances on microscopic pore characteristics of low permeability sandstone reservoirs. Adv Geo-Energy Res 2(2):122–134. https://doi.org/10.26804/ager.2018.02.02

Huang HX, Li RX, Chen WT et al (2021) Revisiting movable fluid space in tight fine-grained reservoirs: a case study from Shahejie shale in the Bohai Bay Basin, NE China. J Pet Sci Eng 207:109170. https://doi.org/10.1016/j.petrol.2021.109170

Huang X, Zhang Y, He MQ, Li X, Yang WP, Lu J (2022) Asphaltene precipitation and reservoir damage characteristics of CO_2 flooding in different microscopic structure types in tight light oil reservoirs. Fuel 312:122943. https://doi.org/10.1016/j.fuel.2021.122943

Ji ZM, Zhao J, Chen XL, Gao Y, Xu L, He C, Ma YB, Yao CJ (2022) Three-dimensional physical simulation of horizontal well pumping production and water injection disturbance assisted CO_2 huff and puff in shale oil reservoir. Energies 15(19):7220. https://doi.org/10.3390/en15197220

Jin L, Hawthorne S, Sorensen J, Pekot L, Bosshart N, Gorecki C, Harju J (2017) Utilization of produced gas for improved oil recovery and reduced emissions from the Bakken formation. In: SPE Health, Safety, Security, Environment, and Social Responsibility Conference-North America. OnePetro. https://doi.org/10.2118/184414-MS

Lang DJ, Lun ZM, Lyu CY, Wang HT, Zhao QM, Sheng H (2021) Nuclear magnetic resonance experimental study of CO_2 injection to enhance shale oil recovery. Pet Explor Dev 48(3):603–612. https://doi.org/10.11698/PED.2021.03.15

Lei H, Yang S, Zu L, Wang Z, Li Y (2016) Oil recovery performance and CO_2 storage potential of CO_2 water-alternating-gas injection after continuous CO_2 injection in a multilayer formation. Energy Fuels 30(11):8922–8931. https://doi.org/10.1021/acs.energyfuels.6b01307

Lescure BM, Claridge EL, (1986) CO_2 foam flooding performance vs. Rock wettability. In: SPE Annual Technical Conference and Exhibition. Society of Petroleum Engineers, New Orleans, Louisiana, USA. https://doi.org/10.2118/15445-MS

Li AF, Ren XX, Wang GJ, Wang Y, Jiang K (2015) Characterization of pore structure of low permeability reservoirs using a nuclear magnetic resonance method. J China Univer Pet (ed Nat Sci) 39(6):92–98. https://doi.org/10.3969/j.issn.1673-5005.2015.06.012

Parsons RW (1966) Permeability of idealized fractured rock. SPE J 6(02):126–136. https://doi.org/10.2118/1289-PA

Qu GZ, Su J, Zhao M, Bai XJ, Yao CJ, Peng J (2022) Optimizing composition of fracturing fluids for energy storage hydraulic fracturing operations in tight oil reservoirs. Energies 15(12):4292. https://doi.org/10.3390/en15124292

Song ZJ, Song YL, Li YL, Bai BJ, Song KP, Hou JR (2020) A critical review of CO_2 enhanced oil recovery in tight oil reservoirs of North America and China. In: SPE/IATMI Asia Pacific Oil and Gas Conference and Exhibition. Bali, Indonesia. https://doi.org/10.2118/196548-MS

Tran S, Yassin MR, Eghbali S, Doranehgard MH, Dehghanpour H (2021) Quantifying oil-recovery mechanisms during natural-gas huff'n'puff experiments on ultratight core plugs. SPE J 26(01):498–514. https://doi.org/10.2118/200341-PA

Wang GC, Locke CD (1980) A laboratory study of the effects of CO_2 injection sequence on tertiary oil recovery. Soc Pet Eng J 20(04):278–280. https://doi.org/10.2118/7953-PA

Wang RF, Shen PP, Song ZQ, Yang H (2009) Characteristics of micropore throat in ultra-low permeability sandstone reservoir. Acta Pet Sin 30(4):560–563, 569. https://doi.org/10.7623/syxb200904014

Wang XW, Yang ZM, Li HB, Guo HK (2010) Experimental study on pore structure of low permeability core with NMR spectra. J Southwest Pet Univer (sci Technol Ed) 32(2):69. https://doi.org/10.3863/j.issn.1674-5086.2010.02.013

Wang C, Gao H, Gao Y, Fan HM (2020) Influence of pressure on spontaneous imbibition in tight sandstone reservoirs. Energy Fuels 34(8):9275–9282. https://doi.org/10.1021/acs.energyfuels.0c00639

Wang M, Dong L, Chen F, Dong WZ (2022) Study on the optimization of injection modes and injection parameters for natural gas in ultra-low permeability reservoir. Energy Rep 8:232–238. https://doi.org/10.1016/j.egyr.2022.03.114

Yang XP, Zhao WZ, Zou CN, Chen MJ, Guo YR (2007) Origin of low-permeability reservoir and distribution of favorable reservoir. Acta Pet Sin 28(4):57–61. https://doi.org/10.7623/syxb200704011

Yang H, Li SX, Liu XY (2013) Characteristics and resource prospects of tight oil and shale oil in Ordos Basin. Acta Pet Sin 34(1):1–11. https://doi.org/10.7623/syxb201301001

Yao YB, Liu DM (2012) Comparison of low-field NMR and mercury intrusion porosimetry in characterizing pore size distributions of coals. Fuel 95:152–158. https://doi.org/10.1016/j.fuel.2011.12.039

Yao YB, Liu DM, Cai YD, Li JQ (2010) Advanced characterization of pores and fractures in coals by nuclear magnetic resonance and X-ray computed tomography. Sci China Earth Sci 53(6):854–862. https://doi.org/10.1007/s11430-010-0057-4

Yao CJ, Liu BS, Liu YQ, Zhao J, Lei ZD, Wang Z, Li L (2022) Quantitative investigation on natural gas flooding characteristics in tight oil cores after fracturing based on nuclear magnetic resonance technique. SPE J 27(06):3757–3772. https://doi.org/10.2118/212835-PA

Zou CN, Zhu RK, Wu ST, Yang Z, Tao SZ, Yuan XJ, Hou LH, Yang H, Xu CC, Li DH, Bai B, Wang L (2012) Types, characteristics, genesis and prospects of conventional and unconventional hydrocarbon accumulations: taking tight oil and tight gas in China as an instance. Acta Pet Sin 33(2):173–187. https://doi.org/10.7623/syxb201202001